Single spacecraft nulling interferometer for exoplanets – Preliminary concepts

Jérôme Loicq[1,2], Denis Defrère[3], Romain Laugier[3], Rudolf Saathof[1], Jasper Bouwmeester[1], Pierre Piron[1], Sandra Potin[1], Colin Dandumont[2], Vincent Moreau[4], Benoit Borguet[4], Pascal Hallibert[5], David Alaluf[5], Isabel Escudero[5], Theresa Lueftinger[5], Bertrand Mennesson[6], William Danchi[7].

[1]**Faculty of Aerospace Engineering, Delft University of Technology,** 2629 HS Delft, The Netherlands, [2]**Université de Liège**, STAR Institute, Liège, Belgium, [3]**KULeuven**, Institute of Astronomy, Leuven, Belgium, [4]**AMOS**, Liege Science Park, Angleur, Belgium, [5]**European Space Agency, ESTEC,** 2200 AG Noordwijk, The Netherlands, [6]**Jet Propulsion Laboratory,** Pasadena, CA, USA, [7]**NASA Goddard Space Flight Center**, Exoplanets, Stellar Astrophysics Laboratory, Greenbelt, MD, USA.

ABSTRACT

One of the most ambitious goals of modern astronomy is to uncover signs of extraterrestrial biological activity, primarily achieved through spectroscopic analysis of light emitted by exoplanets to identify specific atmospheric molecules. Most exoplanets are indirectly identified through techniques like transit or Doppler shift of the host star's flux. Long-term surveys have yielded statistical insights into the occurrence rates of different planet types based on factors such as radius/mass, orbital period, and the spectral type of the host star. Initial estimates of terrestrial planets within the habitable zone have also emerged. However, the difficulty of detecting light from these exoplanets leaves much unknown about their nature, formation, and evolution. As the number of rocky exoplanets around nearby stars rises, questions about their atmospheric composition, evolutionary trajectory, and habitability increase. Direct measurement of an exoplanet's atmospheric composition through its spectral signature in the infrared can provide answers. Measuring the infrared spectrum of these planets poses significant challenges due to the star/planet contrast and very small angular separation from their host stars. Previous research showed that space-based telescopes are mandatory, and unless large primary mirrors (>30m in diameter) can be sent into space, interferometric techniques become essential. Combining light from distant telescopes with interferometric techniques allows access to information at minimal angular separation, operating within the diffraction limit of individual telescopes. Successful demonstrations of on-ground nulling interferometry open a new era for such space-based missions. They are vital to sidestep and tackle these scientific questions. We recently initiated a new study with the European Space Agency to explore the design parameters and the performances related to an interferometric concept based on a single spacecraft and sparse multiple sub-apertures. Launch constraints are linked to the use of an Ariane 6 launch vehicle. Our parametric study covers a range of 1-4 m for the diameter of the telescope and a 10-60 m baseline. The most promising concept working in the infrared range (3-20μm) will be highlighted. This study is conducted by TUDelft in cooperation with KULeuven, CSL/ULiège, and Amos with the support of the European Space Agency.

Keywords: Nulling interferometry, exoplanets, direct imaging, spaceborne,

1. INTRODUCTION

Since the discovery of the first exoplanet around a main-sequence star [1], the field of exoplanet science has been growing rapidly, and more than 10.000 exoplanets and exoplanet candidates have now been discovered. The vast majority of these exoplanets were indirectly identified, via the periodic dimming (transit technique) or the Doppler shift (radial velocity technique) of the host star flux. Thanks to the statistics derived from long-term surveys, both from the ground (such as, the HARPS survey or the California Planet Survey) and from

Optical and Infrared Interferometry and Imaging IX, edited by Jens Kammerer, Stephanie Sallum, Joel Sanchez-Bermudez, Proc. of SPIE Vol. 13095, 1309536
 · 0277-786X · doi: 10.1117/12.3018998

Space (e.g., NASA's Kepler and TESS missions), we now have a first quantitative understanding of the occurrence rate of different planet types as a function of their radius/mass, orbital period and also the spectral type of the host star. In addition, we also have first estimates of the occurrence rate of terrestrial planets lying within the habitable zone (HZ) of their host stars. However, because the direct light emitted or reflected from these exoplanets is generally not detected, very little is currently known about their nature, formation, and evolution. Today, as the number of rocky exoplanets discovered around our nearest stellar neighbours increases rapidly [2] questions about the nature of these worlds are asked more than ever before. What is the atmospheric composition of these planets? How did they evolve? Are they habitable? How common is a planet like Earth? Are we alone? Are we unique? What successions of events lead to the emergence and survival of life?

To address these questions, the consensus among the exoplanet community is that this will require an ambitious space-based direct imaging instrument able to characterise the atmospheric properties of a statistically significant sample of terrestrial exoplanets. Following the ”voyage 2050” call, the senior committee of ESA recommended the “characterisation of the Temperate exoplanets”: “Answering the question of the existence and distribution of life elsewhere in the Universe has been an important driver for the exploration of other worlds, both in and outside of our Solar System.” This theme is one of the top three priorities for future large ESA missions (L-Class missions).

The mid-infrared regime provides strong absorption bands of several molecules such as H20, CO2, O3, N2O, NH3, and CH4. These molecules, known as biosignatures, although indicative of potential life, can also be produced by abiotic processes. Nevertheless, their detections in the spectrum point to habitability and will lead to more specific research on the target. The mid-infrared regime also better constrains the atmospheric structure and composition of Earth-like planets and permits the determination of planetary radius. [3].

However, measuring the infrared spectrum of a rocky exoplanet is an extremely challenging task due to the high contrast and small angular separation between a planet and its host star. For instance, the Sun is 10^7 times brighter than the Earth at 10 μm and separated by only 0.1 arcseconds at full elongation, if located at 10 parsecs. Due to the overwhelming thermal background and the absorbing molecules associated with our Earth's atmosphere a space-based telescope will be required to observe a significant number of terrestrial exoplanets, and unless giant primary mirrors (>30m in diameter) can be launched into space, interferometric techniques will be mandatory to tackle this observational challenge. By combining the light from distant telescopes, interferometric techniques provide a way to access very small angular information by observing directly within the diffraction limit of individual single-dish telescopes.

In 1978, Bracewell [4] proposed a space-based interferometer with two apertures and recombination of light in phase opposition. It produces a dark fringe on the line-of-sight and the stellar emission is strongly suppressed. For an off-axis source, the light can be transmitted depending on the baseline length and the wavelength, which define the interferometer transmission map. While most technical and scientific studies related to space-based high-contrast interferometry stopped after 2007, the field of high-precision ground-based interferometers has recently seen significant progress both in Europe and the United States. In particular, Europe has gained substantial expertise in the field of fringe sensing, tracking, and stabilization with the operation of the *Very Large Telescope Interferometer* (VLTI). This maturity contributed to the first direct observation of an exoplanet with long-baseline interferometry, providing record-breaking precision on the astrometry (and hence mass) and spectrum of any directly imaged planet to date [5]. In parallel, ground-based mid-infrared nulling interferometers have reached record-breaking contrasts down to a few 10-4 [6]. In the laboratory, the Adaptive Nuller [7] has shown that mid-infrared nulls of 10^{-5} are achievable with a mean wavelength of 10 μm. Another testbed, the Planet Detection Testbed [8], was developed in parallel and demonstrated the main components of a high-performance four-beam nulling interferometer at a level matching that needed for the space mission. At

10 μm, it has achieved nulling of $8x10^{-6}$ (the flight requirement is 10^{-5}), starlight suppression of 10^{-8} after post-processing, and actual planet detection at a planet-to-star contrast of $3x10^{-7}$, i.e., the Earth-Sun contrast.

Even though the nulling interferometry principle was demonstrated on the ground on different telescopes and in the laboratory, a space-based mission is needed to avoid atmospheric effects (turbulence and opacity at specific wavelengths). To tackle this technological challenge, the Swiss Federal Institute of Technology in Zurich (ETH) initiated the Large Interferometer For Exoplanets[1] (LIFE) [9]. Although a sizable interferometric mission is the Grail of exoplanetary research/seeking, the challenges represented by such a project are pretty vast and require preparatory work to make a multi-spacecraft mission successful. Such a mission requires formation flying, which induces a high level of risk by its nature and increased complexity, especially for controlling the optical beam at the nm level.

This paper explores the possible architectures that can be implemented on a single spacecraft with the highest scientific return. One of the main constraining requirements is driven by the spacecraft's launch, which limits the size of the interferometer due to the fairing of the rocket. In this study it is required the use of Ariane 6 by the ESA. Various configurations are being analyzed, with already encouraging results regarding the detection of exoplanets. In addition, this study can be considered as a preliminary step towards mitigating risks for future multi-spacecraft-based nulling interferometry missions.

2. ARCHITECTURE IDENTIFICATION

While the basic principles of nulling interferometry are straightforward, the complexity arises from the multitude of parameters characterizing such an interferometer. One of the key elements is the general architecture, which determines the symmetries of the transmission map and consequently the detection efficiency of the interferometer. The relationship between the transmission map and interferometer performance is well-documented in the literature [10]–[12]. Formation flying offers the advantage of large possible baselines and the ability to reconfigure the pupil array, allowing the optimization of the transmission map based on the target. In contrast, a single-spacecraft system, though restricting the overall system dimensions, provides better control and stability of the optical beams and simplifies the coarse pointing of the pupil. While a single spacecraft system inherently manages the relative pupil alignment, formation flying requires independent adjustments of the relative positions of the telescope spacecraft, leading to higher propellant consumption, that will induce higher weight, risks and cost. By its nature, a single spacecraft is easier to position and spin around the line of sight, while the amplitude of the baseline adjustment is limited. Figure 1 describes the different possibilities identified for a single spacecraft.

[1] See LIFE website for more information : https://www.life-space-mission.com/

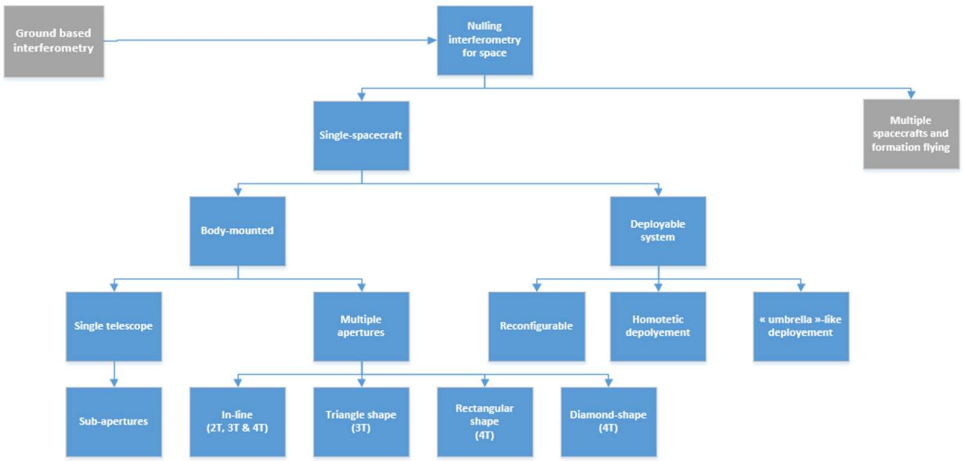

Figure 1: Summary of the nulling interferometry concepts useful for space and under study.

The performance of an array configuration must be considered in conjunction with the beam combination architecture and the observing strategy. Several combination schemes will leverage different features of the array geometry.

- In a **single Bracewell** [4] the beam combination can provide a null depth measurement, which is a high-contrast proxy to the squared visibility of the scene. It is sensitive to symmetrical features of the object. Consequently, the detection of a planet will retain a 180° degeneracy, the signal from a resolved star or a centre-symmetric exozodiacal light will result in a background signal. Simultaneous nulling of multiple all pairs of apertures is possible to obtain more information, at the cost of spreading the light on more detectors.
- A **double-Bracewell configuration** with its staged combination, can leverage four apertures to give a pair of complementary dark outputs. Since most instrumental noises (due to the fluctuation of the optical paths and the throughput) are correlated on these outputs, computing their difference results in a differential null which is more stable. The internal modulation by a phase shift of π effectively operates a permutation of the two dark outputs, essentially offering additional opportunities for bias subtraction. This differential output is sensitive to asymmetric features of the target. Depending on the permutation of the inputs, three different asymmetric responses can be obtained, which are comparable to the closure phases one would obtain with the same array of apertures.
- **Kernel-nullers** are a generalised form of combiners producing such differential observables. One version of this for four inputs would produce all three pairs of outputs mentioned above at the same time [13]. Combination from three inputs (one pair of outputs) to six inputs (ten pairs of outputs) have been proposed [14] and practical configurations for some of them have been described and examined in the context of LIFE [15]–[18]. However, the real advantages of such configurations come into play for lifting degeneracies in some model-fitting parameters, or in the fitting of multiple-planet models, which has not been a part of previous studies.

A rotation of the array around the line of sight has been the prevalent solution proposed to compensate for the

small number of observables, as it helps to fill the coverage of the UV plane. Despite this, significant correlations are expected between the different parameters of a model fit, particularly between photometry and astrometry, which will be one of the key performance parameters to compare architectures. A relatively fast rotation (several revolutions per hour) may be interesting to circumvent the temporal spectrum of instrumental errors, and provide high-quality measurements. This will be less costly to achieve with a single structure compared to individual spacecraft flying in formation.

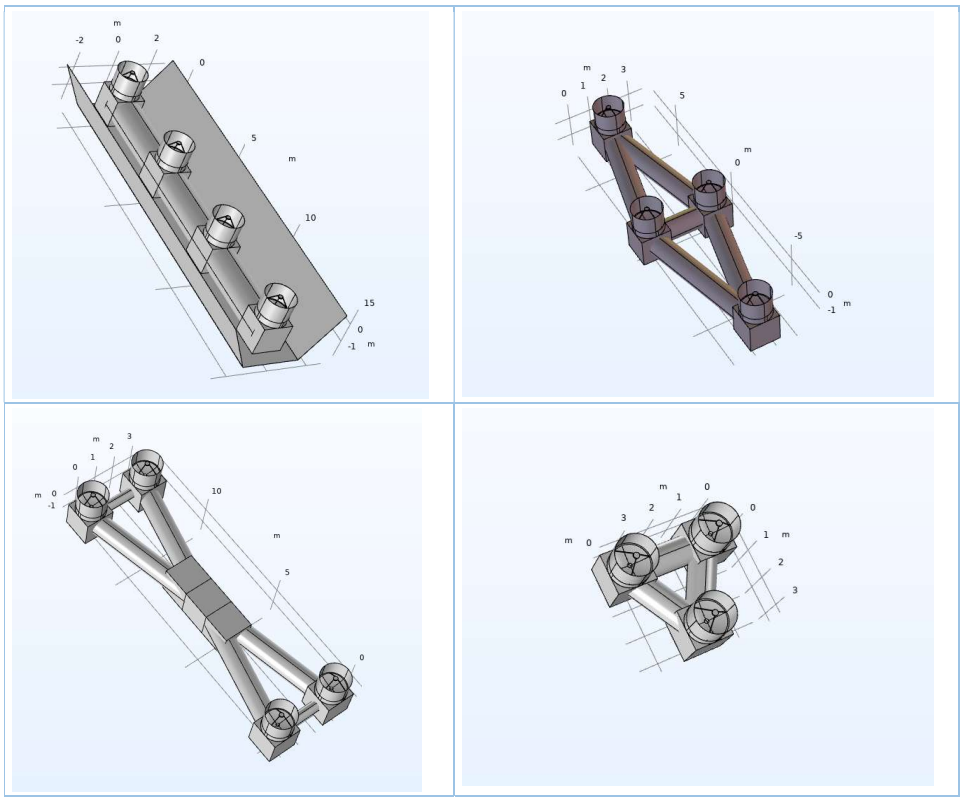

Figure 2: Examples of nulling interferometry architectures under study by the consortium for large spacecraft.

When developing a nulling interferometer, it is vital to have a deep understanding of the various parameters that govern the system and affect its overall performance. Table 1 below highlights the main parameters and their impacts.

Table 1: Driving parameters of a single S/C nulling interferometer

Driving Parameters	**Impact on Performance**
Baseline Length	Affects the angular resolution and the inner working angle.
Diameter of the Telescopes	Influences the field of view and interferometer sensitivity by affecting the amount of light collected.
Number of Telescopes and Geometrical Configuration	Determines the system's imaging capabilities, including UV plane coverage, and helps resolve source ambiguities (e.g., exozodiacal disks, asymmetry, multiple exoplanets).

Payload Temperature	Affects sensitivity by reducing the thermal background noise and determines the wavelength range.
Optical Beam Control	Impacts contrast, influencing null depth and stability, sensitivity by suppressing starlight
Phase Shifting	Impacts the contrast, leading to starlight suppression.
Array Rotation Around the Line of Sight	Improves contrast and enhances imaging capabilities through better UV plane coverage, and self-calibration of static errors (by providing a known modulation to the signal)
Spectral Resolution	Allows the identification of specific spectroscopic line features, effective temperature and the chemical composition of observed objects.
Integration Time	Influences sensitivity, longer times increase the signal-to-noise ratio.
Cost	Determines the scale of the mission, including the number and diameter of telescopes, affecting overall performance and feasibility.

3. OPTICAL CHAIN

As the first iteration of the optical chain, we propose the following configuration (see Figure 3). This scheme presents the sequence of each of the arms of the interferometer. The building blocks are described below. The number of telescopes, N, depends on the architecture. A Bracewell configuration corresponds to N = 2 while it can be larger in case of a sparse aperture telescope.

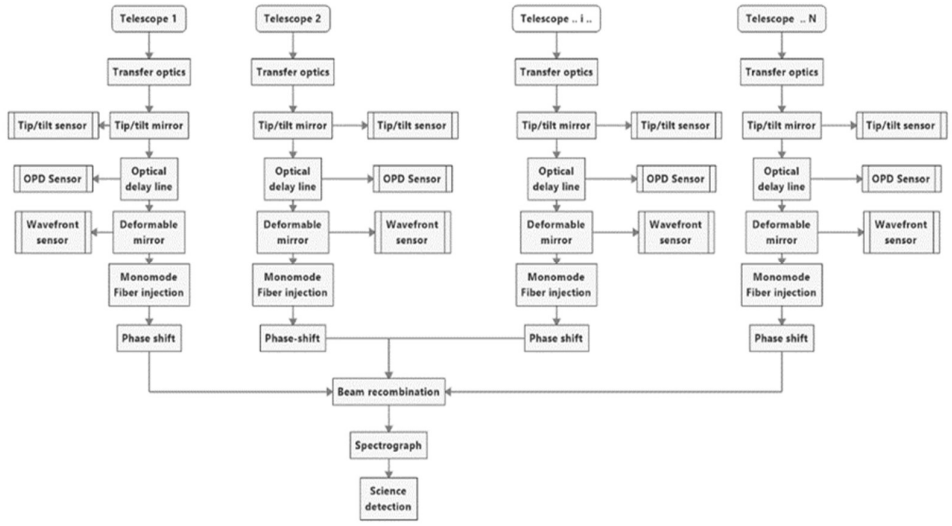

Figure 3: First iteration optical chain.

One of the initial optical configurations for the interferometer is a four-telescope configuration (referred to as X-array). Essential technologies for the nulling interferometer include:

a. **Telescope assembly & transfer optics:** Each arm necessitates a telescope assembly to gather light from the target, offering design flexibility including siderostat or plane mirror, afocal telescope, or focussing telescope options. Transfer optics then direct and shape the light for further processing.

b. **Beam control and compensations:** This involves (i) Tip/tilt mirrors for correcting beam deviations, utilising fast steering mirrors and control loops; (ii) Active optics mirrors to address optical aberrations and quasi-static errors, with deformable mirrors adjusting light intensity and shape at the entrance of single-mode fibres for optimal coupling efficiency; (iii) Correction loop & wavefront sensor, utilising a closed loop system where a wavefront sensor converts errors into physical deformations corrected by deformable mirrors; (iv) Optical delay lines units to adjust Optical Path Differences (OPD) between arms due to vibrations and thermal variations; (v) Nulling control system (fringe tracker) ensuring interferometer nulling by measuring fringes (contrast) and providing feedback to optical delay lines.

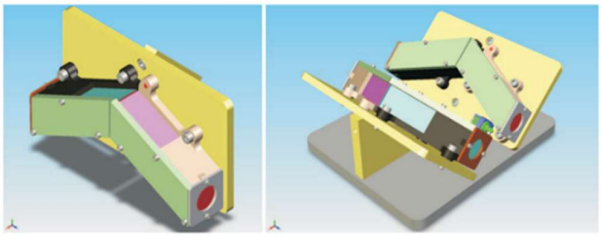

Figure 4: Broadband achromatic phase shifter (Darwin Legacy) [19]

c. **Optical fiber injection unit:** The optical fibre injection unit plays a crucial role in nulling interferometry by filtering optical aberrations, enabling deep nulls. Various methods like single-mode fibre optics, photonic crystal fibres, or integrated optics can achieve spatial filtering across wide bandwidths.

d. **APS unit**: In each arm, an appropriate achromatic phase shifter covering the entire waveband (3-18 µm) introduces a phase delay to create destructive interference in the line of sight [20].

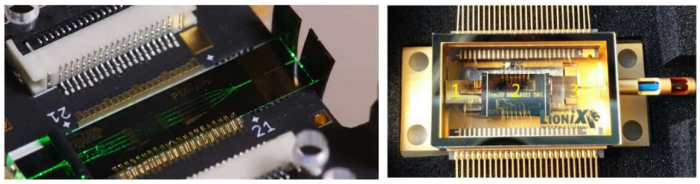

Figure 5: Lionix photonics integrated circuit – beam combiner [21], [22]

e. **Beam combiner unit:** The beam combiner, essential for creating interference in the pupil plane, must accommodate various apertures; our project will design and build the interferometer configurations based on Mach-Zehnder and photonic nullers.

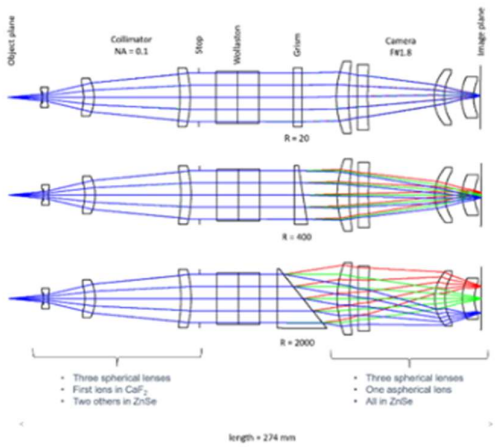

Figure 6: Optical design of the Multiple-resolution Asgard/NOTT spectrograph in the VLTi [23], [24].

f. **Spectrograph:** At the end of the optical chain, light will be separated into multiple spectral channels with the aim of a spectrograph. Within the framework of the Asgard/Nott instrument for the VLTi, a compact Ge-Grism-based in-line spectrograph has been designed to operate at multiple infrared spectral bands and resolution [23], [24]. This spectrograph will be the basis of the space-based spectrograph nuller.

g. Science detection assembly: The detectors must operate within the 1-20 μm infrared wavelength range, gathering light from the interferometer's multiple outputs.

4. PRELIMINARY RESULTS

One of the most critical metrics for evaluating the performance of any exoplanet-seeking instrument is its capability to detect exoplanets and, ideally, characterize their spectral properties. To facilitate this assessment, the ETH Zurich (ETHZ) group has developed an open-source tool named LIFESim [25], [26]. This tool is invaluable for evaluating the number of exoplanets detectable in various rectangular interferometer configurations. LIFESim is closely integrated with P-pop, a planet population synthesis tool devised by Kammerer and Quanz [27], which leverages data from the Kepler satellite. P-pop simulates synthetic populations of exoplanets orbiting nearby main-sequence stars within a distance of 20 parsecs. By using this simulated exoplanet population, LIFESim allows us to model and analyze the performance of the interferometer, including its ability to detect exoplanets and derive their spectral characteristics, thereby providing a robust framework for optimizing interferometer design and observational strategies.

Figure 7 illustrates the preliminary results generated by LIFESim for a single-spacecraft (S/C) interferometer configuration. This graph focuses on a 30-meter X-array interferometer equipped with 2-meter class telescopes. The detection phase simulations indicate that such a system can observe over 240 exoplanets within a 4-year observational program. Notably, approximately 10% of these detected exoplanets are predicted to be rocky, and potentially Earth-like planets.

Figure 8 demonstrates the impact of the primary mirror size on the detection capabilities of the interferometer. Analyzing the data reveals that, on average, increasing the telescope diameter by 1 meter leads to a 40% increase in the number of detectable exoplanets. This significant improvement can be attributed to the enhanced light-gathering power that larger mirrors provide. Larger primary mirrors enable the detection of fainter and more distant exoplanets by capturing more photons from these objects, thereby improving the signal-to-noise ratio in the observations. The trade-off between mirror size and other system parameters, such as mission cost and spacecraft design constraints, must be carefully evaluated to maximize the scientific return of the mission.

The findings presented in Figure 7 and Figure 8 highlight the interplay between interferometer architecture and observational capabilities, providing valuable insights for the design and optimization of future exoplanetary detection missions. These results illustrate the importance of considering both interferometric configuration and primary mirror dimensions in developing efficient and effective exoplanet-seeking instruments.

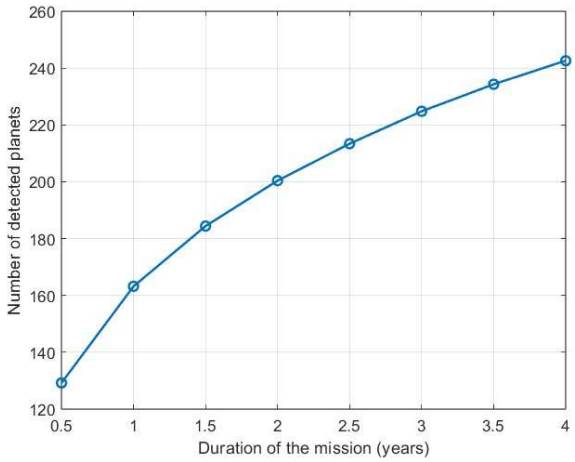

Figure 7: Number of detected planets for a rectangular interferometer with a nulling baseline of 30 m and an edge ratio of 0.5, four telescopes of 2m diameter, waveband: 3-20 µm, spectral resolution is 20, Optical throughput = 10 %, QE = 70%.

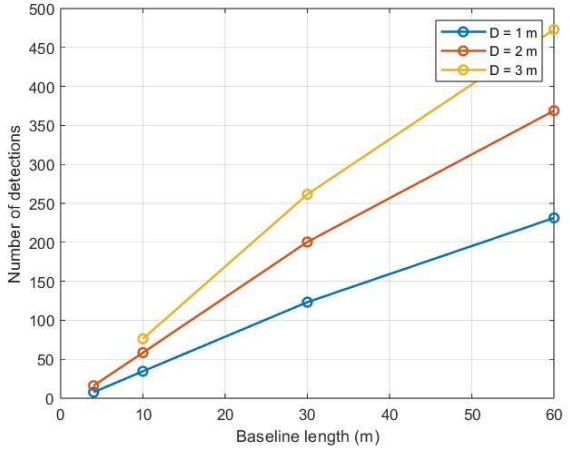

Figure 8: Impact of the size of the dishes on the exoplanet detection number (2 years mission).

5. CONCLUSION

Characterizing exoplanets is critical for advancing our understanding of planetary systems and the potential for life beyond Earth. Interferometry is now routinely used in ground-based astronomical instruments. Additionally, nulling interferometry, effectively employed or under development by facilities such as LBTI and VLTI, shows great promise for detecting and characterizing exoplanets, particularly in the habitable zone. For example, a 30-meter baseline X-array interferometer with 3-meter diameter telescopes could lead to the detection of more than 450 exoplanets within a 2-year mission.

The importance of characterizing temperate exoplanets in the habitable zone is highlighted in ESA's Voyage 2050 report, which identifies it as a priority for future L-Class missions. The ESA's senior committee emphasized this endeavor, noting that understanding the existence and distribution of life elsewhere has driven the exploration of worlds both within and beyond our Solar System. The report advocates for the development of mid-infrared (MIR) observatories, which will complement the objectives of ongoing missions like PLATO, ARIEL, and HWO.

In addition to a standalone mission with a real scientific detection yield, the study presented in this paper is also a crucial initial step toward mitigating risks for future multi-spacecraft-based nulling interferometry missions. Achieving such an interferometric mission is an ambitious goal, requiring extensive preparatory efforts to address challenges like formation flying and precise control of optical beams at the nanometer scale.

*j.j.d.loicq@tudelft.nl.

6. REFERENCES

[1] M. Mayor and D. Queloz, “A Jupiter-mass companion to a solar-type star,” *Nature*, vol. 378, no. 7, p. 355, 1995.
[2] G. Anglada-Escudé *et al.*, “A terrestrial planet candidate in a temperate orbit around Proxima Centauri,” *Nature*, vol. 536, no. 7617, pp. 437–440, 2016, doi: 10.1038/nature19106.
[3] D. Defrère *et al.*, “Space-based infrared interferometry to study exoplanetary atmospheres,” *Exp. Astron.*, vol. 46, no. 3, pp. 543–560, 2018, doi: 10.1007/s10686-018-9613-2.
[4] R. N. Bracewell, “Detecting Nonsolar Planets by Spinning Infrared Interferometer,” *Nature*, vol. 274, no. 5673, pp. 780–781, 1978, doi: 10.1038/274780a0.
[5] S. Lacour *et al.*, “First Direct Detection of an Exoplanet by Optical Interferometry,” *Astron. Astrophys.*, vol. 623, p. L11, 2019.
[6] D. Defrère *et al.*, “Simultaneous water vapor and dry air optical path length measurements and compensation with the large binocular telescope interferometer,” *Opt. Infrared Interferom. Imaging V*, vol. 9907, p. 99071G, 2016, doi: 10.1117/12.2233884.
[7] R. D. Peters, O. P. Lay, M. Jeganathan, and A. Hirai, “Adaptive Nulling for the Terrestrial Planet Finder Interferometer Outline • Background • How it works • Development activities • Summary,” 2006.
[8] S. Martin, A. Booth, K. Liewer, N. Raouf, F. Loya, and H. Tang, “High performance testbed for four-beam infrared interferometric nulling and exoplanet detection,” *Appl. Opt.*, vol. 51, no. 17, pp. 3907–3921, 2012, doi: 10.1364/AO.51.003907.
[9] P. S. P. Quanz, “Atmospheric characterization of terrestrial exoplanets – habitability , biosignatures and diversity,” 2019.
[10] J. T. Hansen, M. J. Ireland, R. Laugier, and the L. collaboration, “Large {{Interferometer For Exoplanets}} ({{LIFE}}): {{VII}}. {{Practical}} Implementation of a Kernel-Nulling Beam Combiner with a Discussion on Instrumental Uncertainties and Redundancy Benefits,” no. arXiv:2204.12291. arXiv, 2022.
[11] O. P. Lay, “Imaging properties of rotating nulling interferometers,” *Appl. Opt.*, vol. 44, no. 28, pp. 5859–5871, 2005, doi: 10.1364/AO.44.005859.
[12] O. Guyon, B. Mennesson, E. Serabyn, and S. Martin, “Optimal Beam Combiner Design for Nulling Interferometers,” *Publ. Astron. Soc. Pacific*, vol. 125, no. 930, pp. 951–965, 2013, doi: 10.1086/671816.

[13] F. Martinache and M. J. Ireland, “Kernel-nulling for a robust direct interferometric detection of extrasolar planets,” *Astron. Astrophys.*, vol. 619, pp. 1–10, 2018, doi: 10.1051/0004-6361/201832847.
[14] R. Laugier, N. Cvetojevic, and F. Martinache, “Kernel Nullers for an Arbitrary Number of Apertures,” *Astron. Astrophys.*, vol. 642, p. A202, 2020, doi: 10.1051/0004-6361/202038866.
[15] J. T. Hansen and M. J. Ireland, “A linear formation-flying astronomical interferometer in low Earth orbit,” *Publ. Astron. Soc. Aust.*, pp. 1–10, 2020, doi: 10.1017/pasa.2020.13.
[16] J. T. Hansen and M. J. Ireland, “Large Interferometer For Exoplanets (LIFE): IV. Ideal kernel-nulling array architectures for a space-based mid-infrared nulling interferometer,” *Astron. Astrophys.*, vol. 664, pp. 1–13, 2022, doi: 10.1051/0004-6361/202243107.
[17] M. J. Ireland, “Long-baseline space interferometry for astrophysics: a forward look at scientific potential and remaining technical challenges,” no. December 2020, p. 89, 2020, doi: 10.1117/12.2563121.
[18] J. T. Hansen *et al.*, “Interferometric beam combination with a triangular tricoupler photonic chip,” *J. Astron. Telesc. Instruments, Syst.*, vol. 8, no. 02, pp. 1–20, 2022, doi: 10.1117/1.jatis.8.2.025002.
[19] D. Mawet *et al.*, “Fresnel rhombs as achromatic phase shifters for infrared nulling interferometry,” *Opt. Express*, vol. 15, no. 20, 2007, doi: 10.1364/OE.15.012850.
[20] P. Gabor *et al.*, “Tests of achromatic phase shifters performed on the SYNAPSE test bench: A progress report,” in *Proceedings of SPIE - The International Society for Optical Engineering*, 2008, vol. 7013. doi: 10.1117/12.789269.
[21] C. G. H. Roeloffzen *et al.*, “Low-loss si3n4 triplex optical waveguides: Technology and applications overview,” *IEEE J. Sel. Top. Quantum Electron.*, vol. 24, no. 4, 2018, doi: 10.1109/JSTQE.2018.2793945.
[22] P. Munoz *et al.*, “Foundry Developments Toward Silicon Nitride Photonics from Visible to the Mid-Infrared,” *IEEE J. Sel. Top. Quantum Electron.*, vol. 25, no. 5, pp. 1–15, 2019, doi: 10.1109/JSTQE.2019.2902903.
[23] C. Dandumont, A. Mazzoli, V. Laborde, R. Laugier, A. Bigioli, and G. Garreau, “Technical requirements and optical design of the Hi-5 spectrometer,” vol. 4.
[24] D. Defrère *et al.*, “plans status and plans,” no. August, 2022, doi: 10.1117/12.2627953.
[25] F. A. Dannert *et al.*, “Large Interferometer For Exoplanets (LIFE) I. Improved exoplanet detection yield estimates for a large mid-infrared space-interferometer mission,” *Astron. Astrophys.*, vol. 21, 2022, doi: 10.1051/0004-6361/202141958.
[26] F. A. Dannert *et al.*, “Large Interferometer For Exoplanets (LIFE). II. Signal simulation, signal extraction, and fundamental exoplanet parameters from single-epoch observations,” *Astron. Astrophys.*, vol. 21, 2022, doi: 10.1051/0004-6361/202141958.
[27] J. Kammerer and S. P. Quanz, “Simulating the exoplanet yield of a space-based mid-infrared interferometer based on Kepler statistics,” *Astron. Astrophys.*, vol. 609, pp. 1–14, 2018, doi: 10.1051/0004-6361/201731254.